JTTEE5
DOI: 10.1007/s11666-014-0211-1
1059-9630/$19.00 © ASM International



# Dielectric Breakdown Strength of Thermally Sprayed Ceramic Coatings: Effects of Different Test Arrangements

*Minna Niittymäki, Kari Lahti, Tomi Suhonen, and Jarkko Metsäjoki*

*(Submitted July 4, 2014; in revised form November 12, 2014)*

**Dielectric properties (e.g., DC resistivity and dielectric breakdown strength) of insulating thermally sprayed ceramic coatings differ depending on the form of electrical stress, ambient conditions, and aging of the coating, however, the test arrangements may also have a remarkable effect on the properties. In this paper, the breakdown strength of high velocity oxygen fuel-sprayed alumina coating was studied using six different test arrangements at room conditions in order to study the effects of different test and electrode arrangements on the breakdown behavior. In general, it was shown that test arrangements have a considerable influence on the results. Based on the results, the recommended testing method is to use embedded electrodes between the voltage electrode and the coating at least in DC tests to ensure a good contact with the surface. With and without embedded electrodes, the DBS was 31.7 and 41.8 V/μm, respectively. Under AC excitation, a rather good contact with the sample surface is, anyhow, in most cases acquired by a rather high partial discharge activity and no embedded electrodes are necessarily needed (DBS 29.2 V/μm). However, immersion of the sample in oil should strongly be avoided because the oil penetrates quickly into the coating affecting the DBS (81.2 V/μm).**

**Keywords** $Al_2O_3$, breakdown strength, coating, dielectric, HVOF, thermal spraying

## 1. Introduction

Thermally sprayed ceramic coatings, such as alumina and magnesium aluminate, can be utilized as an electrical insulation in demanding conditions (e.g., in harsh environments or in high-temperature applications) where normal insulating materials, such as polymers, cannot be used. However, relatively few studies on the dielectric properties of thermally sprayed ceramic coatings can be found in literature which makes this area of research interesting and necessary. In order to be able to design electrical insulation systems based on thermally sprayed ceramics, the electrical performance of these materials must be known. The performance is defined by dielectric parameters (e.g., permittivity, tan δ, resistivity, and breakdown strength) which are, anyhow, not constant values but differ depending on the form of electrical stress (e.g., DC, AC, frequency of AC, transients) and ambient conditions (such as temperature, humidity) and also the aging of a material (long-term properties). Arrangements during tests and measurements may affect the results remarkably. Due to the above reasons, the measurements of dielectric parameters are typically made according to standards, like IEC 60243-1 or ASTM D 149-09(2013) for dielectric breakdown strength. Although a certain standard is used, there are often several details which may vary between separate tests. In the case of breakdown measurements, for example, different voltage application methods and electrode configurations may be used as well as different insulating mediums may be used around the test sample to prevent surface arcing and flashovers over the sample. Since details of test arrangements may have an effect on the test results, tests shall always be documented in detail and comparisons between the results of different tests shall be made with careful consideration (Ref 1, 2).

Because of the spraying process, the microstructure of thermally sprayed coating consists of splats, voids, cracks, and different kinds of defects due to which thermally sprayed coatings have some degree of porosity. Increased porosity decreases the dielectric breakdown strength of thermally sprayed ceramic coating (Ref 3, 4). Typically, insulating solid ceramics is less porous than the thermally sprayed coatings. Due to this, solid ceramics may usually be tested as immersed in insulating oil to prevent flashovers over the sample surface, because the oil will not easily penetrate inside the material structure and thus affect the test results. Most of the previous studies on insulating ceramics are focused on the electrical properties of solid alumina which has different microstructural properties than thermally sprayed coatings, and due to this direct comparison between the dielectric properties of solid and thermally sprayed materials is not reasonable. Quite many of the breakdown strength measurements of

**Minna Niittymäki** and **Kari Lahti**, Tampere University of Technology, Tampere, Finland; and **Tomi Suhonen** and **Jarkko Metsäjoki**, VTT Technical Research Centre of Finland, Espoo, Finland. Contact e-mail: minna.niittymaki@tut.fi.



Published online: 01 January 2015

the solid ceramics are made using AC voltage (50 or 60 Hz), but the dielectric breakdown strength measurements of ceramic coatings are typically performed using DC voltage in air without oil immersion (Ref 3-16).

As it was mentioned earlier, the used electrode configuration may have influence on the dielectric breakdown results. In Ref 3, 17-19 the breakdown measurements of thermally sprayed ceramic coatings were performed without silver-painted or other way embedded electrodes on sample surface, but in Ref 4, 5 silver-painted electrodes were used to improve the contact between the steel electrode and the coating. The effect of steel electrode shape was studied for solid alumina in Ref 11, and a ball-shaped electrode was recommended. The ball-shaped electrode arrangement is also introduced in the IEC standard 60672-2, but since it requires a ball-shaped hole to be machined in the sample to be tested and as a consequence of this a rather thick sample is required, this method is not in practice applicable to thermally sprayed coatings (Ref 20). However, when a ball-shaped electrode is used, the electric field distribution over the tested area is more homogenous, and thus it is a more preferable electrode arrangement for breakdown testing. On the other hand, the tested area is really small since the maximal field strength is present only at the vicinity of the head of the ball electrode. Due to this, a rather high deviation of results can be expected in Ref 20 with this arrangement and as a consequence, a large number of parallel tests are needed in order to get a realistic view of the breakdown distribution over the large areas of a material. Actually, the IEC Standard 60672-2 recommends using a test method where a ball-shaped hole is not machined in the sample.

The breakdown test results of thermally sprayed ceramics are usually presented as an average value from five to ten parallel measurements (Ref 3-5, 17, 18). Typically, breakdown data of solid ceramics are also presented as Normal distribution values (mean and standard deviation), but in Ref 11 the weakest link failure analysis was used in a case of solid alumina, and the results were analyzed statistically with two distributions: Weibull and Laplace. The latter was reported to agree better than Weibull. In typical solid electrical insulations (e.g., polymers), Weibull analysis is normally performed for breakdown data if the parallel measurements of more than 10 are made (Ref 11, 21, 22).

In this paper, the breakdown strength of one type of high velocity oxygen fuel (HVOF)-sprayed aluminum oxide coating is studied with several different test arrangements at room temperature conditions. The breakdown measurements are performed with silver-painted electrodes and without any embedded electrodes in air and in oil mainly with DC voltage. Statistical analysis, such as Normal and Weibull distributions, are performed for the breakdown data. The measurement methods are documented in detail, and the effect of electrode arrangements as well as the effect of insulation oil immersion is analyzed. The dependence between the coating microstructure and the breakdown strength is also discussed.

**Table 1 Main spray parameters**

| Parameter | |
|---|---|
| Spray distance, mm | 170 |
| Gas parameters, L/min | |
| $H_2$ | 700 |
| $O_2$ | 350 |
| $N_2$ | 20 |
| Sweeps, pcs | 15 |
| Scanning step size, mm | 4 |
| Relative torch scan velocity, m/s | 1 |

## 2. Experimental

### 2.1 Studied Material

Commercial fused high purity $Al_2O_3$-powder (99.9 wt. %, Praxair) was deposited on carbon steel substrate by high velocity oxygen fuel (HVOF) spraying method. The particle size of the powder was from 5 to 22 μm which is a very suitable size for HVOF process. The used HVOF gun was HV2000 (Praxair), and the main spray parameters are listed in Table 1. The coating was tested as sprayed without any polishing, grinding, or sealing because a sealer can fill the voids of the coating, thus affecting the results (Ref 3).

The porosity values of the studied coating were defined by image analysis from optical micrographs (OM) with image magnification of 320 and using scanning electron microscope (SEM) micrographs taken with two detectors: secondary electron detector (SE) and backscattered electron detector (BSE) both with image magnification of 1000. The porosity values were defined by three OM images and by two SEM images. Five parallel surface roughness measurements were made with 2D-profilometer along the coating surface.

### 2.2 Sample Preparation

DC resistivity, relative permittivity, and breakdown strength measurements were made at the temperature of 20 °C and at the relative humidity of 45%. These conditions were maintained in the big climate room of TUT High voltage laboratory where all the measurement actions were made at the above-mentioned ambient conditions. At first, the samples were preconditioned at 120 °C for 2 h and then stabilized at 20 °C and RH 45% for 12 h before the measurements. For DC resistivity and relative permittivity measurements, a round silver electrode (∅ = 50 mm) was painted on the middle of a coating sample before preconditioning. In addition, a shield electrode was painted around the measuring electrode to neglect possible surface currents. For some of the breakdown measurements, silver electrodes (∅ = 11 mm) were painted on the samples before preconditioning. Silver paint penetration was studied from cross-sectional optical micrographs. It was observed that the used paint (SPI Conductive Silver Paint) did not penetrate into the coating.

### 2.3 DC Resistivity and Relative Permittivity of the Studied Material

DC resistivity was studied at three different electric field strengths because some thermally sprayed ceramic coatings have shown non-ohmic behavior already at quite low electric fields (Ref 18). DC resistivity measurements were made using Keithley 6517B electrometer. The test voltage was maintained until a stabilized current level (i.e., pure resistive current) was reached. In practice, the tests were performed at test voltages ranging from 10 to 30 V, and the stabilized DC current was measured approximately 1000 s after the voltage application. The DC resistivity was calculated using the mean value of the stabilized current at 998-1000 s, the test voltage, and the sample thickness. All the measurement arrangements were in accordance with the standards IEC 60093 or ASTM D257-07 (Ref 23, 24).

Relative permittivity and dielectric losses of the material were studied with an insulating diagnosis analyzer device (IDA 200). During the measurements, a sinusoidal voltage with varying frequency was applied across the sample. The measuring voltage was 200 $V_{peak}$ corresponding to the electric field of 1.5 $V_{peak}/\mu m$.

The complex impedance of a sample was expressed by IDA device as an equivalent parallel RC circuit model and calculated from the measured test voltage and the current through a sample. The relative permittivity ($\varepsilon_r$) and dissipation factor (tan δ) were calculated from the measured parallel resistance and capacitance using Eq 1, 2, where $C_p$ is the measured parallel capacitance and $R_p$ the parallel resistance of the equivalent circuit model of the dielectric. $C_0$ is the so-called geometric capacitance of the test sample (vacuum in place of the insulation) and ω is the angular frequency. The edge field correction ($C_e$) was not used in these measurements because a shield electrode was utilized in the measurements. All the test arrangements were performed in accordance with the IEC standard 60250 (Ref 25).

$$\varepsilon_r \approx \varepsilon_r' = \frac{C_p}{C_0} - \frac{C_e}{C_0} \quad \text{(Eq 1)}$$

$$\tan\delta = \frac{1}{R_p C_0 \omega}. \quad \text{(Eq 2)}$$

Loss index ($\varepsilon_r''$) includes all the losses of a sample: both conductive and dielectric ones (as well as the dissipation factor). It can be defined from relative permittivity and dissipation factor, tan δ, using Eq 3.

$$\varepsilon_r'' = \varepsilon_r \tan\delta. \quad \text{(Eq 3)}$$

### 2.4 Breakdown Measurements

During the breakdown tests, the samples were clamped between two stainless steel electrodes: a rod (∅ = 11 mm) and a flat plate (∅ = 50 mm). The used rod electrode was flat-ended and edge-rounded with a radius of 1 mm. Schematic figure of this measurement bench is illustrated in Fig. 1(b). Some of the measurements were made with a graphite felt disk electrode (∅ = 11 mm, the thickness of 0.76 mm) placed in between the stainless steel rod electrode and the coating, and some of the measurements were made in oil immersion with "Shell Diala oil DX Dried" insulation oil.

Breakdown measurements were made using six different measuring arrangements:

(1) at DC voltage in air without oil immersion or painted electrodes on coating surface
(2) at DC voltage in oil immersion without painted electrodes
(3) at DC voltage with silver-painted electrodes (∅ = 11 mm) in air
(4) at DC voltage with graphite disk electrodes (∅ = 11 mm) in air
(5) at DC voltage with silver-painted electrodes (∅ = 11 mm) in oil
(6) at AC voltage (50 Hz) in air without oil immersion or painted electrodes.

All the breakdown voltage measurements were made with linearly ramped DC or AC voltage. Software-controlled linear ramp rate of 100 V/s was used in all tests. In oil measurements, the ramp rate of the voltage was started 30 s after the sample was immersed in the oil. The schematic figure of the measurement circuit is presented in Fig. 1(a). The used DC voltage source was Spellman

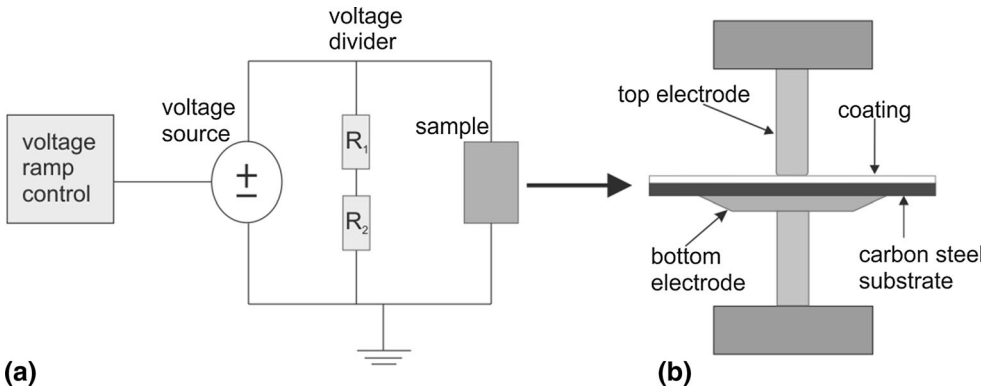


**Fig. 1** (a) Measurement circuit of the breakdown measurements and (b) schematic figure of the measurement bench where the sample is clamped between the rod electrode and the larger flat electrode

SL1200 ($U_{max} = 130$ kV). In the DC measurements, the voltage divider was Spellman HVD 100-1 resistive voltage divider ($U_n = 100$ kV and scale factor 10000:1). The used AC voltage source was Hipotronics test transformer ($U_{max,rms} = 50$ kV), and the measured voltage was recorded directly from the high voltage side of the transformer. After each test, a confirmation was made to check that a breakdown had occurred, not a flashover along the surface of the coating.

After the measurements, the thicknesses of samples without silver-painted electrodes were measured at the point right next to the breakdown points to define exactly the dielectric breakdown field strength of each breakdown point. For the samples with silver-painted electrodes, the thickness of each coating was measured before painting the silver electrodes. The thicknesses were measured with a magnetic measuring device (Elcometer 456B).

In DC tests, the dielectric breakdown strength of a coating, $E_b$, was calculated by dividing the measured breakdown voltage, $V$, by the corresponding thickness of the breakdown point, $d$, (Eq 4). In AC tests, the dielectric breakdown strength was calculated by dividing the measured peak value of the measured AC voltage by the thickness of the measurement point since the peak value of the ac-based breakdown strength is comparable to the DC dielectric breakdown strength.

$$E_b = \frac{V}{d}. \quad \text{(Eq 4)}$$

### 2.5 Statistical Analysis of Breakdown Data

The mean value and experimental standard deviation of Normal distribution can be easily calculated from dielectric breakdown strength data. However, typically the electrical breakdown data of solid insulations are Weibull, Gumbel, or log-normal distributed. These distributions can be used reliably only if at least 10 parallel tests are made because less test results are not statistically relevant enough. Typically, Weibull distribution is used to analyze the breakdown voltage data of solid insulations. This distribution is a one of the extreme value distributions which means that the system fails when the weakest link of the system fails. The cumulative density function of a two-parameter Weibull distribution is given in Eq 5:

$$F(t, \alpha, \beta) = 1 - \exp\left\{\left(\frac{t}{\alpha}\right)^{\beta}\right\}, \quad \text{(Eq 5)}$$

where $F(t)$ is the breakdown probability, $t$ is the measured breakdown strength (V/μm), $\alpha$ is the scale parameter (V/μm), and $\beta$ is the shape parameter (V/μm). Both $\alpha$ and $\beta$ are positive values. The scale parameter represents the breakdown strength at the 63.2% failure probability and it is analogous to the mean of Normal distribution. The shape parameter is a measure of the range of failure voltages. Larger $\beta$ means that the range of breakdown voltages is smaller. $\beta$ is analogous to the inverse of standard deviation of the Normal distribution (Ref 21, 22).

Weibull parameters can be estimated in different ways such as using Maximum Likelihood estimation (MLE) and rank-regression methods. The statistical analysis was performed using Weibull++ software, and the Maximum Likelihood method was used in the parameter estimation.

## 3. Results

### 3.1 Properties of the Studied Coating

The mean porosity values of the studied HVOF coating are listed in Table 2. They were defined by image analysis from optical micrographs and by scanning electron microscope (SEM) micrographs taken with two detectors: secondary electron (SE) and backscattering electron (BSE). A cross-section surface image of the studied HVOF-sprayed $Al_2O_3$ coating is shown in Fig. 2 where the darker spots are pores and voids. The typical lamellar microstructure of thermally sprayed ceramic coating can be seen in Fig. 2. The substrate of the coating was grit blasted before spraying to enhance the attachment of the coating which, anyhow, has an effect on the thickness deviation of the coating (Fig. 3a). A cross-section image taken by optical microscope is shown in Fig. 3(b) where the rough substrate surface can obviously be seen. The thickness variation of the coating (minimum = 89 μm, average = 115 μm) is also illustrated in Fig. 3(b). The mean value of the surface roughness, $R_a$, is 2.7 μm with a standard deviation of 0.15 μm which is a typical value for HVOF-sprayed coatings.

**Table 2 Porosity of the studied coating**

| Measurement method | Magnification | Average porosity, % | SD, % |
|---|---|---|---|
| optical micrographs | ×320 | 1.4 | 0.1 |
| SEM/SE | ×1000 | 1.1 | 0.5 |
| SEM/BSE | ×1000 | 2.2 | 0.2 |

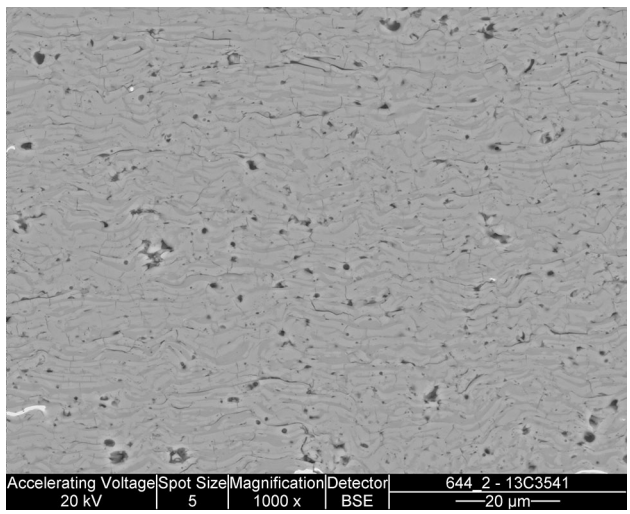


**Fig. 2** Cross-section figure of the studied coating taken by SEM/BSE

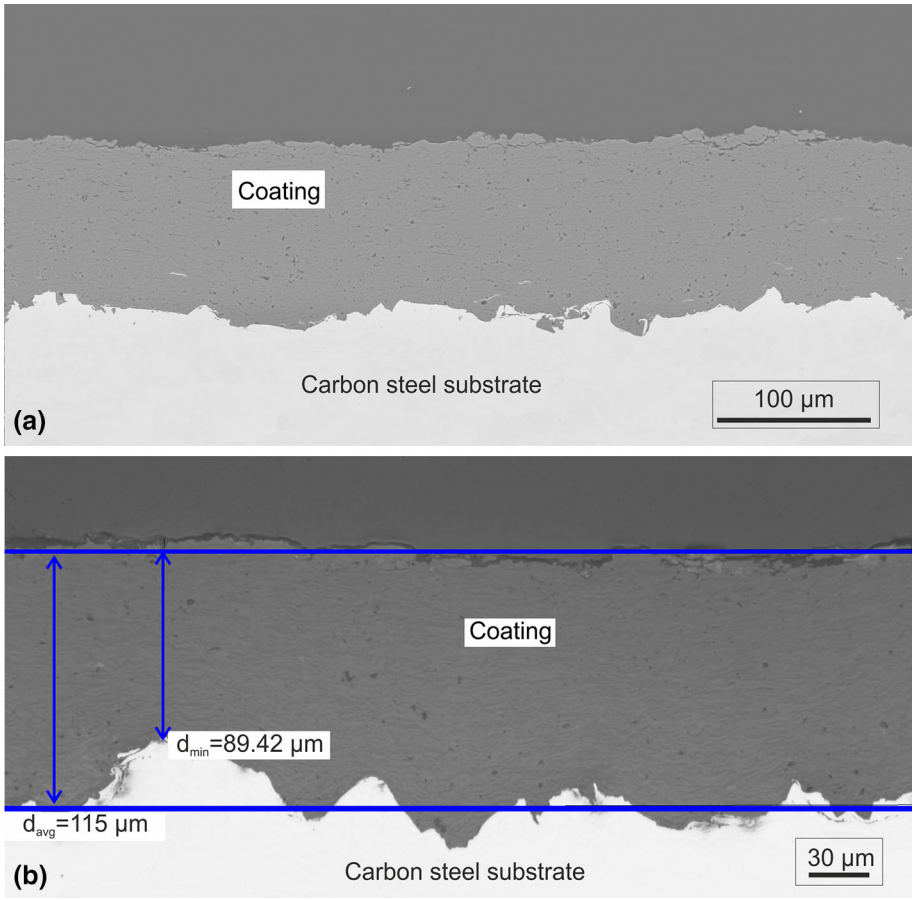


**Fig. 3** (a) Cross-section figure of the studied coating taken by SEM/BSE. (b) Cross-section figure of the studied HVOF coating taken by optical microscope. Thickness variation is marked in the figure; 89.42 µm is the lowest value and 115 µm is the average value

**Table 3 DC resistivity of the studied material at low electric field strengths ($T$ = 20 °C, RH 45%)**

| Thickness, µm | Voltage, V | Electric field, V/µm | Resistivity, Ωm |
|---|---|---|---|
| 92 | 10 | 0.11 | 4.66E+12 |
| | 20 | 0.22 | 3.80E+12 |
| | 30 | 0.33 | 1.12E+12 |

### 3.2 DC Resistivity and Relative Permittivity

Low field DC resistivities of the studied alumina coatings are given in Table 3. In author's previous studies, the resistivity of HVOF alumina was $9 \times 10^{12}$ Ωm at the electric field of 0.5 V/µm (thickness 279 µm), and the resistivity of HVOF spinel was $2.9 \times 10^{12}$ Ωm at the electric field of 0.5 V/µm (Ref 17, 18). Thus, the resistivity values obtained in this paper are at a similar level compared to the previous studies. The relative permittivity and the loss index of the studied material at various frequencies are given in Table 4; measured values are lower than in author's previous studies (HVOF alumina, 279 µm), presumably due to the different raw materials and the different sample thickness (Ref 17).

**Table 4 Relative permittivity of the studied material at various frequencies, the RMS value of the measuring voltage was 140 V which corresponds to the electric field of 1.5 $V_{rms}$/µm ($T$ = 20 °C, RH 45%)**

| Frequency, Hz | Relative permittivity, $\varepsilon_r$ | Loss index, $\varepsilon_r''$ |
|---|---|---|
| 1 | 10.4 | 1.94 |
| 10 | 8.5 | 0.93 |
| 50 | 7.9 | 0.50 |
| 100 | 7.7 | 0.37 |
| 1000 | 7.4 | 0.16 |

### 3.3 Dielectric Breakdown Strength

Fifteen parallel breakdown measurements for the HVOF-sprayed alumina coating were made with each of the six different test arrangements mentioned in Chapter 2. The mean values of the dielectric breakdown strengths and the corresponding experimental standard deviations were calculated and are presented in Table 5 and Fig. 4. The deviation of dielectric breakdown strength between parallel measurements was quite large with all the arrangements. The thickness variation of the samples is also listed in Table 5, where the mean and standard

**Table 5 Average dielectric breakdown strength of 15 parallel measurements and experimental standard deviations in different test arrangements as well as Weibull parameters and the breakdown probabilities at 10 and 90% failure probability ($T = 20$ °C, RH 45%)**

| Voltage form | Test arrangement | Mean thickness, µm | SD, µm | Average DBS, V/µm | SD, V/µm | Weibull, parameters | | | |
|---|---|---|---|---|---|---|---|---|---|
| | | | | | | α, V/µm | β | DBS, V/µm at probability 10% | DBS, V/µm at probability 90% |
| DC | Dry | 114 | 3.0 | 41.8 | 8.1 | 44.9 | 6.6 | 32.0 | 51.0 |
| DC | Dry + silverpaint | 116 | 3.2 | 31.7 | 5.8 | 34.0 | 6.4 | 23.9 | 38.8 |
| DC | Dry + graphite | 115 | 3.9 | 37.1 | 4.5 | 39.1 | 8.6 | 30.1 | 43.1 |
| DC | Oil | 111 | 5.0 | 81.2 | 20.2 | 89.0 | 4.3 | 52.7 | 108.1 |
| DC | Oil + silverpaint | 114 | 4.1 | 45.5 | 7.2 | 48.3 | 8.5 | 37.0 | 53.3 |
| AC | Dry | 114 | 4.4 | 29.2 | 6.0 | 31.5 | 6.1 | 21.8 | 36.2 |

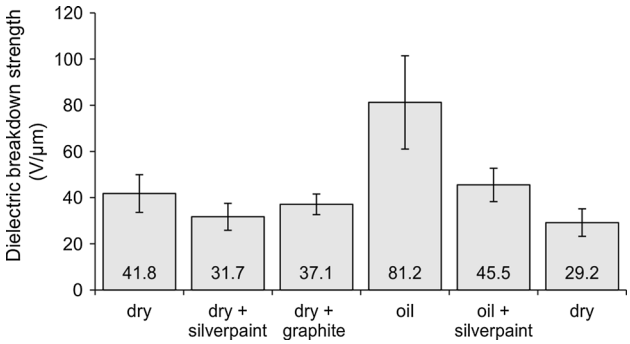


**Fig. 4** Average dielectric breakdown strength with different test arrangements. The error bars show the experimental standard deviations

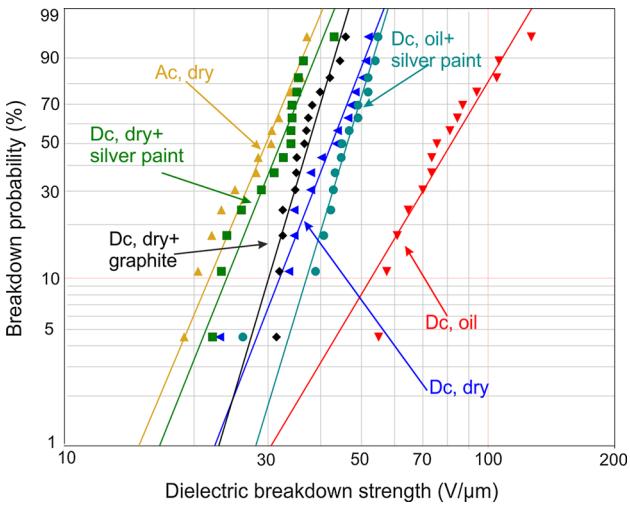


**Fig. 5** Weibull distributions with different test arrangements: AC dry, DC dry, DC dry with silver-painted electrodes, DC dry with graphite electrodes, DC oil, and DC oil with silver-painted electrodes

deviation of 15 measured breakdown point thicknesses are shown. Weibull parameters α (the breakdown field at the failure probability of 63.2%) and β (shape parameter) of the breakdown measurements are also presented in

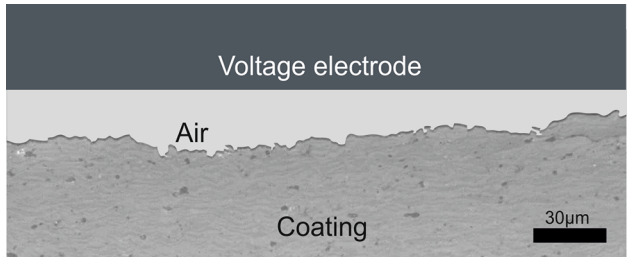


**Fig. 6** Formed air gap between the voltage electrode and the tested coating during the breakdown measurements

Table 5 along with the breakdown field values at the breakdown probabilities of 10 and 90%. Better comparison between different test arrangements can be made using Weibull distributions illustrated in Fig. 5, where all the breakdown events are shown. Probability of breakdown is shown in *y*-axis, and the dielectric breakdown strength is in *x*-axis.

As it can be seen from the results, large variation of breakdown strength results was depending on the test arrangement used. Anyhow, the differences in the results are well understandable. In DC tests, the lowest result (31.7 V/µm) was obtained with the air-insulated arrangement with embedded silver paint electrodes. In this way, the whole electrode area (∅ = 11 mm) is truly tested in each individual breakdown test. In other words, the weakest point of the breakdown strength distribution over the tested area is measured in this case. Due to the same reason, it is also understandable that the deviation of the results is one of the smallest in this case. The deviation of thickness measured along the electrode area has an effect on the breakdown strength results but this will be discussed in detail in Chapter 4.

However, a 44% higher result (45.5 V/µm) was obtained with otherwise exactly similar test arrangements except that the whole test setup was placed in the oil. The reason for the remarkable increase is most probably that the oil had enough time to penetrate into the coating and fill the voids and pores of the coating even though the breakdowns occurred approximately 1 min 30 s after the sample was immersed in the oil. Breakdown strength of transformer oil is clearly higher (~100 V/µm) than that of

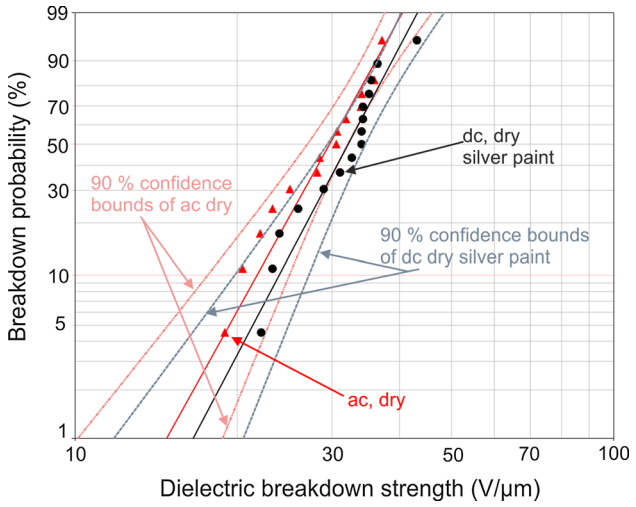


**Fig. 7** Comparison between the results of AC breakdown test in air and the DC test with silver-painted electrodes in air

air or $Al_2O_3$ coatings (Ref 26, 27). It may be assumed that the breakdown path develops in dry conditions through the air-filled pores and voids in the coating. When the voids are filled with highly insulating oil, the breakdown strength of the oil-impregnated coating will increase.

When the breakdown test was made without any embedded electrode on the coating surface, the steel electrode will contact only some of the highest points of the coating, as illustrated in Fig. 6. Evidently, those contact points will be tested in parallel with test arrangements of this kind, and the weakest point will cause the breakdown. In this case, there is air between the steel electrode and the coating surface, and partial discharges will take place in this volume above a certain field strength defined by Paschen's law (Ref 26). The plasma channel of an electrical arc is well conductive, and in this way the point of coating where partial discharge takes place will be tested as well. Since partial discharges will "bombard" the surface of the coating rather intensively (this way testing most of the area of the coating under the electrode) especially in the case of AC voltage stress, it is understandable that the result obtained with this arrangement at AC test voltage (29.2 $V_{AC,peak}$/μm) was close to the result obtained with DC voltage with the silver-painted electrodes (see Fig. 7). In the case of DC excitation, the partial discharge repetition rate is typically much lower (Ref 26, 28), which is probably at least one of the reasons for the higher result in that case (41.8 V/μm). In the case of lower partial discharge activity, the smaller area will be "bombarded" and tested. Also, in this case, the test voltage has time to increase to a higher level before discharge arc takes place at a point weak enough to cause breakdown.

However, in the case where a piece of graphite felt disk (∅ = 11 mm) was placed between the steel rod electrode and the coating, the breakdown strength (37.1 V/μm) was between the case of silver-painted electrodes and the case of steel electrode in air. The graphite felt is a slightly soft allowing better contact with the highest points of the coating than the stainless steel electrode itself. Due to this, the tested area is larger than in the case without any embedded electrode but the area is still smaller than in the case with silver-painted electrodes.

When the air gap between stainless steel electrode and the coating is filled with a well insulating medium like transformer oil, no partial discharges will take place and only the contact points of electrode and the coating will be tested. Understandably, a significantly higher breakdown strength (81.2 V/μm) and deviation of the results were measured with this test arrangement.

## 4. Discussion

When measuring the breakdown voltage of an insulating material, several parameters such as the rate of raise and frequency of the test voltage, specimen thickness, electrode material, configuration, and attachment as well as temperature affect the dielectric breakdown strength. Humidity and aging of the material typically also affect the results (Ref 21).

In Ref 4, 5, silver-painted electrodes were used, and the dielectric breakdown strength of HVOF-sprayed alumina was reported to be 34 V/μm for 120 μm coating and 22 V/μm for 200-210 μm coating at room temperature ambient, while 31.7 V/μm was now measured with the same electrode arrangements for 116 μm thick samples at a temperature of 20 °C and relative humidity of 45%. In author's previous studies (Ref 17), a test procedure with air-insulated steel electrode without embedded contacts was used, and an average dielectric breakdown strength of 31.3 V/μm (SD = 2.1 V/μm) was measured for HVOF-sprayed alumina (thickness of 270 μm) at a temperature of 20 °C and relative humidity of 20%. In this study, the mean value with similar arrangements was 41.8 V/μm ($T$ = 20 °C/RH = 45%, 116-μm sample). The thicker sample partly explains the difference although the ambient humidity was now higher, and the raw material as well as the spraying parameters was different than in the previous study. Anyhow, it can be concluded that the results obtained in this study are in line with the above-mentioned earlier studies.

### 4.1 Effect of Thickness

In Ref 3, 4, it was discussed that the increased amount of voids, cracks, and other defects in the ceramic coating probably decreases the dielectric breakdown strength. The unideal features of the coating are normally the weakest points, and thus increased amount of those decreases the materials' capability to withstand high voltages. Because the microstructure of thermally sprayed coating consists of voids, splats, and pores forming lamellar structure (Fig. 2), the breakdown channel probably forms along the voids. Thus, the breakdown channel might be longer than the measured thickness. In Ref 6, 16, the effect of direction and actual length of breakdown channel through an alumina ceramic material on the breakdown strength has

been discussed. The formation of the breakdown channel in the coating microstructure is an interesting detail, but from the definition of a breakdown strength, it is clear that the breakdown strength of a material must be calculated using the perpendicular thickness of a coating.

In general, the thickness of an insulating material has an effect on the breakdown field strength of material, and thinner samples have typically higher breakdown strengths than thicker ones. There are several reasons for this, partly dependent on breakdown mechanism. In the case of electro thermal breakdown mechanism, the thinner insulation will withdraw heat easier resulting in higher breakdown field strength. From a more general statistical point of view, according to the so-called enlargement law, there is a higher probability to have weak points in larger volume of insulating material due to which the breakdown will take place with higher probability in a case of thicker or larger insulation. This enlargement law is generally expressed mathematically as a power-law relationship (Eq 6) where the exponent, $n$, has to be determined for each material composition separately ($E$ is electric strength and $d$ is the thickness of the sample) (Ref 22, 26, 29).

$$E_2 = E_1\left(d_2/d_1\right)^{-n}. \quad \text{(Eq 6)}$$

In Ref 8, the influence of thickness on the AC breakdown strength of solid alumina ceramics was studied, and an empirical equation was defined based on the measured data for breakdown strength calculation for ceramics with the thickness of 0.7-3.5 mm (Eq 7) ($V_b$ is the breakdown voltage, $t$ is the thickness of the sample). The idea of evolution law is that the results with different thicknesses are comparable when all the results are calculated for 3-mm-thick insulation using Eq 7. This empirical equation is also used in other studies of breakdown strength of solid alumina, but in the previous studies of thermally spayed coatings, the calculations of breakdown strength are made according to Eq 4 without any thickness corrections. In any case, these empirically defined equations shall be used with careful consideration.

$$E_b = \frac{V_b}{t}\sqrt{\frac{t}{3}}. \quad \text{(Eq 7)}$$

The thickness of a coating can be defined either from cross-section figures or with magnetic measuring device. Cross-section figures are usually taken only from a certain small section of a sample. When several breakdown measurements are made from several samples (although all sprayed at the same time, the same method and the same powder), it might be that the thickness of the coating at the breakdown point is not the same what was defined from cross-section figure. Also, from the cross section of the studied material (Fig. 3b), it can be seen that the actual coating thickness varied more than 25 μm in the small area depending on where the value was defined. Because of this variation of thickness, in this paper, the measurements were made with magnetic measuring device at each breakdown point. Due to the measuring principle, the thickness measured with magnetic measuring device is always an average value over a rather small area. This kind of local but averaged thickness measurement is one practical and good way (together with the cross section) to define the thickness. Anyhow, it is clear that the rather high local deviation of thickness will cause remarkable deviation and error in the individual breakdown field results. This fact underlines the need to make large number of parallel measurements to average the individual errors.

Because the silver paint penetrates even into the deepest notches of the surface, the actual breakdown path (thickness) most probably starts from one of these notches. The ball-shaped head of the magnetic thickness measurement device does not fit into these small notches. This might result in a situation where the device gives the thicknesses mainly comparable to the peaks or the average of the surface roughness deviation of a sample. The measured values were, in practice, the only usable thickness values for breakdown strength calculations. Due to the above-mentioned facts, the defined breakdown strength results for this setup are, on average, most probably to some extent too small.

### 4.2 Effect of Oil

Oil immersion is often used in breakdown measurements to avoid flashovers on the sample surface, and it has been used in several solid alumina measurements (Ref 6-9, 11, 14-16). In Ref 11, two different insulation oils were compared in the breakdown measurements of solid alumina ceramic, which porosity and gas permeability was zero, unlike in thermally sprayed ceramics. Thus, in these cases, the use of oil is reasonable because the tested materials have not had open porosity so that the oil could penetrate into the ceramics. Anyhow, care shall be taken to avoid oil layers between the electrodes and the ceramic.

Typical thermally sprayed coating consists of voids, splats, and unmelted particles, i.e., there is some porosity in the coating (Fig. 2). Because of the porosity of the ceramic coatings, the oil penetrates very quickly into the coating and fills the voids when the sample is placed in the oil bath. The breakdown strength of the insulation system of oil and alumina coating is significantly higher than alumina coating. Thus, it can be concluded that the oil immersion is not a recommended measurement method for the breakdown testing of thermally sprayed ceramics.

However, if the flashovers cause problems while making the breakdown testing and oil immersion is not an option; the sample can be placed only partly in the oil. The idea is that the testing area is dry so that it is isolated from the oil by an insulating cylinder. The cylinder is pressed tightly against a ceramic sample with the help of a rubber O-ring sealing toward the specimen surface. The high voltage rod electrode is placed in the middle of the cylinder and pressed against the ceramic sample. Small amounts of insulation oil can be poured outside this plastic cylinder.

### 4.3 Effect of Electrode Arrangements

In Ref 11, the comparison between stainless steel ball and the cylindrical plate electrodes was made in the

breakdown measurements of alumina at AC voltage and the breakdown strength was higher with ball electrodes. It is well known that when using a ball electrode as a voltage electrode and a spherical hole is machined onto the sample for it, the slight local field enhancement is not formed in the tested area. Due to this, maximum electric field strength is achieved with this test setup (this measurement arrangement is also mentioned in IEC standard 60672-2). However, preparing a spherical hole on coating samples is really laborious which makes it impractical to use this test arrangement with thermally sprayed ceramic coatings. Actually, ASTM Standard D149-09(2013) also recommends using fixed cylindrical electrodes with flat ends which is the commonly used method in the breakdown testing of solid insulating materials.

According to the breakdown testing standard ASTM D149-09(2013), painted electrodes can be used but the painting may affect the results (Ref 1). In this paper, when the silver-painted electrodes were used, the breakdown strength of the alumina coating decreased both in air and oil arrangements, since the whole electrode area was tested and truly the weakest point of the coating over that area was found. In addition, in all the air-insulated arrangements, partial discharge activity has an effect on the tested area, which is discussed in the following. However, the difference between the test results with and without embedded electrodes depends on the variation of the breakdown strength over the electrode area. In the case of a more homogeneous material also the breakdown distribution is, in practice, more homogeneous, and consequently the difference between the results of the test arrangements is smaller.

However, if a graphite disk was used between the voltage electrode and the coating, the breakdown strength was lower than without any embedded electrodes and the deviation was the lowest, indicating that the slightly soft graphite felt improves the contact with the coating. Due to this, larger electrode area will be tested than in the case of steel rod electrode.

### 4.4 Effect of Partial Discharges

As it was discussed earlier, partial discharges occur in dry measurements without any embedded electrodes between the voltage electrode and the coating because an air gap is formed there as shown in Fig. 6. The highest value for air gap is approximately 15 μm in the figure. The breakdown strength of air is presented by Paschen curve as a function of thickness multiplied by air pressure. According to Paschen curve for air at a temperature of 20 °C and in normal air pressure, the breakdown voltage for 15-μm-thick air gap is 450 V (Ref 26).

Partial discharges (pd) obviously affect the breakdown results as shown in this paper by improving the electrical contact with the coating. The pd activity was measured for one of the HVOF samples, and in the case of AC excitation the discharges started at the peak voltage of 1060 V (total electrode voltage) with a repetition rate of approximately 800 discharges per minute. In the DC case, the inception voltage was 1700-2000 $V_{peak}$, and the repetition rate was obviously lower than in the AC case. Due to this difference, the coating withstood higher voltage levels in DC breakdown test (41.8 V/μm) than in AC case (29.2 V/μm) when embedded electrodes were not used. When silver-painted electrodes were used, the whole painted area was continuously tested. Due to this, the breakdown occurred at a lower voltage level (31.7 V/μm) which was actually close to the AC result (29.2 V/μm). Supposing the evidently high pd activity at AC voltage can provide a proper contact over the electrode area, this result also indicates that the polarity of test voltage has no major influence on the results.

## 5. Conclusions

The dielectric breakdown strength of thermally sprayed alumina coating was studied with six various test arrangements. Because thermally sprayed coating is a porous material, the used insulation oil penetrates into pores of the coating as well as between the electrode and coating surface if no coating surface-embedded electrode is used. In practice, this occurs very fast after the sample is placed in the oil bath. Thus, the dielectric breakdown strength of the oil impregnated alumina coating is measured to be 94% higher than without oil immersion. Due to this, oil immersion is not a recommended measurement method for the breakdown testing of thermally sprayed ceramics.

Silver-painted electrodes on the coating surface improve the contact between the stainless steel rod electrode and the coating surface. The tested area is also larger than without any embedded electrodes. In this case, the deepest points on the coating surface are tested so that the weakest point of the painted area is truly found. Due to this, the DC breakdown strength test result is 24% lower than in the case without embedded electrodes.

If embedded electrodes are not used, partial discharges take place between the voltage electrode and the coating improving the contact (test area) between them. Under AC excitation, the partial discharge activity is more extensive than in the DC case resulting in very similar dielectric breakdown strength results than with the coating surface-embedded electrodes. In the DC case, the rather low discharge activity leads to smaller test area and higher breakdown test results. Anyhow, this method can be used to compare different materials but it shall be kept in mind that the obtained breakdown results are probably slightly higher than the results obtained with an arrangement with surface-embedded electrodes.

In the case of silver-painted electrodes on the surface, the typically averaged coating thickness measurement may lead to use of slightly too high thickness and correspondingly too low breakdown strength. In general, the marked variation of the coating thickness is a source of uncertainty and variation of the results. To minimize the uncertainty, a high enough number of parallel measurements is needed, typically at least 10 is preferred.

All the measurement arrangements include imperfections mainly arising from the unsmoothed surfaces of the substrate and the coating. Those could be avoided if coatings were sprayed on a smooth surface, and the coatings were grinded and polished before testing. In practice, thermally spayed coatings cannot be sprayed on completely smooth substrate; however, it might be possible to coat smooth-grinded substrates for breakdown tests if higher accuracy is required. In any case, the use of oil shall be avoided.

In general, among other details the test arrangements of the breakdown tests have a considerable effect on the results gathered. Due to this, care should be taken when evaluating the results obtained in different studies. The full documentation of the test conditions is a necessity.

## References


1. ''ASTM Standard D-149-09(2013) Standard Test Method for Dielectric Breakdown Voltage and Dielectric Strength of Solid Electrical Insulating Materials at Commercial Power Frequencies,'' ASTM International, West Conshohocken, PA, 2013
2. ''IEC Standard 60243-1 Electric Strength of Insulating Materials—Test Methods—Part 1: Tests at Power Frequencies,'' IEC, 2013
3. L. Pawłowski, The Relationship Between Structure and Dielectric Properties in Plasma-sprayed Alumina Coatings, *Surf. Coatings Technol.*, 1988, **35**(3–4), p 285-298
4. F.L. Toma, L.M. Berger, S. Scheitz, S. Langner, C. Rödel, A. Potthoff, V. Sauchuk, and M. Kusnezoff, Comparison of the Microstructural Characteristics and Electrical Properties of Thermally Sprayed $Al_2O_3$ Coatings from Aqueous Suspensions and Feedstock Powders, *J. Therm. Spray Technol.*, 2012, **21**(3–4), p 480-488
5. F.L. Toma, S. Scheitz, L.M. Berger, V. Sauchuk, M. Kusnezoff, and S. Thiele, Comparative Study of the Electrical Properties and Characteristics of Thermally Sprayed Alumina and Spinel Coatings, *J. Therm. Spray Technol.*, 2011, **20**(1–2), p 195-204
6. C. Neusel, H. Jelitto, D. Schmidt, R. Janssen, F. Felten, and G.A.A, Schneider, Dielectric Breakdown of Alumina Single Crystals, *J. Eur. Ceram. Soc.*, 2012, **32**(5), p 1053-1057
7. C. Neusel and G.A. Schneider, Journal of the Mechanics and Physics of Solids Size-Dependence of the Dielectric Breakdown Strength from Nano- to Millimeter Scale, *J. Mech. Phys. Solids*, 2014, **63**(February), p 201-213
8. J. Liebault, J. Vallayer, D. Goeuriot, D. Treheux, and F. Thevenot, How the Trapping of Charges can Explain the Dielectric Breakdown Performance of Alumina Ceramics, *J. Eur. Ceram. Soc.*, 2001, **21**(3), p 389-397
9. M. Touzin, D. Goeuriot, C. Guerret-Piécourt, D. Juvé, and H.-J. Fitting, Alumina Based Ceramics for High-Voltage Insulation, *J. Eur. Ceram. Soc.*, 2010, **30**(4), p 805-817
10. M. Touzin, D. Goeuriot, H.J. Fitting, C. Guerret-Piécourt, D. Juvé, and D. Tréheux, Relationships Between Dielectric Breakdown Resistance and Charge Transport in Alumina Materials-Effects of the Microstructure, *J. Eur. Ceram. Soc.*, 2007, **27**(2–3), p 1193-1197
11. B. Block, Y. Kim, and D.K. Shetty, Dielectric Breakdown of Polycrystalline Alumina: A Weakest-Link Failure Analysis, *J. Am. Ceram. Soc.*, 2013, **96**(11), p 3430-3439
12. J.J. O'Dwyer, Breakdown in Solid Dielectrics, *Electr. Insul. IEEE Trans.*, 1982, **IE-17**(6), p 484-487
13. L. Haddour, N. Mesrati, D. Goeuriot, and D. Tréheux, Relationships Between Microstructure, Mechanical and Dielectric Properties of Different Alumina Materials, *J. Eur. Ceram. Soc.*, 2009, **29**(13), p 2747-2756
14. I.O. Owate and R. Freer, AC Breakdown Characteristics of Ceramic Materials, *J. Appl. Phys.*, 1992, **72**(6), p 2418-2422
15. M. Touzin, D. Goeuriot, H. Fitting, D. Juv, and D. Tr, Relationships Between Dielectric Breakdown Resistance and Charge Transport in Alumina Materials—Effects of the Microstructure, *J. Eur. Ceram. Soc.*, 2007, **27**, p 1193-1197
16. F. Talbi, F. Lalam, and D. Malec, Dielectric Breakdown Characteristics of Alumina, *Proceedings of 2010 International Conference on Solid Dielectrics (ICSD)*, Potsdam, Germany, 2010, p 1–4
17. M. Niittymäki, B. Rotthier, T. Suhonen, J. Metsäjoki, and K. Lahti, Effects of Ambient Conditions on the Dielectric Properties of Thermally Sprayed Ceramic Coatings, *Proceedings of the 23th Nordic Insulation Symposium Nord-IS 2013*, Trondheim, Norway, 2013, p 131–135
18. M. Niittymäki, K. Lahti, T. Suhonen, U. Kanerva, and J. Metsäjoki, Dielectric Properties of HVOF Sprayed Ceramic Coatings, *Proceedings of the IEEE International Conference on Solid Dielectrics*, Bologna, Italy, 2013, p 389–392
19. E. Turunen, T. Varis, S.-P. Hannula, A. Vaidya, A. Kulkarni, J. Gutleber, S. Sampath, and H. Herman, On the Role of Particle State and Deposition Procedure on Mechanical, Tribological and Dielectric Response of High Velocity Oxy-fuel Sprayed Alumina Coatings, *Mater. Sci. Eng. A*, 2006, **415**(1–2), p 1-11
20. IEC standard 60672-2, *Ceramic and Glass Insulating Materials—Part2: Methods of Test*. IEC, 1999
21. IEC 62539, *Guide for the Statistical Analysis of Electrical Insulation Breakdown Data*, IEC, 2007
22. W. Hauschild and W. Mosch, *Statistical Techniques for High-Voltage Engineering*, Lightning Source UK LTd, Milton Keynes, 1992, p 310
23. ''ASTM Standard D257 - 07 Standard Test Methods for DC Resistance and Conductance of Insulating Materials'', ASTM Standard No. D257–07, ASTM International, West Conshohocken, PA, 2007
24. ''IEC Standard 60093 Methods of Test for Volume Resistivity and Surface Resistivity of Solid Electrical Insulating Materials,'' IEC Standard No. 60093, IEC, 1980
25. ''IEC standard 60250 Recommended Methods for the Determination of the Permittivity and Dielectric Dissipation Factor of Electrical Insulating Materials at Power, Audio and Radio Frequencies Including Metre Wavelengths, IEC Standard No. 60250, IEC, 1969
26. E. Kuffel, W.S. Zaengl, and J. Kuffel, *High Voltage Engineering: Fundamentals, Second edi*, Elsevier Ltd, Oxford, 2000, p 539
27. R. Bartnikas, Dielectrics and Insulators, *The Electrical Engineering Handbook, Second Edition*, CRC Press, Boca Raton, 1997
28. P.H.F. Morshuis and J.J. Smit, Partial Discharges at DC Voltage: their Mechanism, Detection and Analysis, *Dielectr. Electr. Insul. IEEE Trans.*, 2005, **12**(2), p 328-340
29. B. Tareev, *Physics of Dielectric Materials*, Mir Publishers, Moscow, USSR, 1979, p 270